

# Modeling forced pool–riffle hydraulics in a boulder-bed stream, southern California

Lee R. Harrison \*, Edward A. Keller

*Department of Earth Science, University of California, Santa Barbara, Santa Barbara, CA 93106, USA*

Received 2 May 2005; received in revised form 13 February 2006; accepted 13 February 2006

Available online 11 July 2006

## Abstract

The mechanisms which control the formation and maintenance of pool–riffles are fundamental aspects of channel form and process. Most of the previous investigations on pool–riffle sequences have focused on alluvial rivers, and relatively few exist on the maintenance of these bedforms in boulder-bed channels. Here, we use a high-resolution two-dimensional flow model to investigate the interactions among large roughness elements, channel hydraulics, and the maintenance of a forced pool–riffle sequence in a boulder-bed stream. Model output indicates that at low discharge, a peak zone of shear stress and velocity occurs over the riffle. At or near bankfull discharge, the peak in velocity and shear stress is found at the pool head because of strong flow convergence created by large roughness elements. The strength of flow convergence is enhanced during model simulations of bankfull flow, resulting in a narrow, high velocity core that is translated through the pool head and pool center. The jet is strengthened by a backwater effect upstream of the constriction and the development of an eddy zone on the lee side of the boulder. The extent of flow convergence and divergence is quantified by identifying the effective width, defined here as the width which conveys 90% of the highest modeled velocities. At low flow, the ratio of effective width between the pool and riffle is roughly 1:1, indicating little flow convergence or divergence. At bankfull discharge, the ratio of effective width is approximately 1:3 between the pool and downstream riffle, illustrating the strong flow convergence at the pool head. The effective width tends to equalize again with a ratio of 1:1 between the pool and riffle during a modeled discharge of a five-year flood, as the large roughness elements above the pool become drowned out. Results suggest that forced pool–riffle sequences in boulder-bed streams are maintained by flows at or near bankfull discharge because of stage-dependent variability in depth-averaged velocity and tractive force.

© 2006 Elsevier B.V. All rights reserved.

*Keywords:* Pool–riffle sequence; Velocity reversal; Large roughness elements; Flow modeling; Boulder-bed; Forced pool

## 1. Introduction

### 1.1. Objectives

The mechanisms by which pools and riffles are formed and maintained are fundamental aspects of channel form and process. The majority of previous studies on pool–riffle sequences have investigated alluvial channels that are free to adjust the bed and banks because of the interaction of flow and sediment.

\* Corresponding author. Current address: Department of Earth Science, University of California at Santa Barbara, Building 526, Santa Barbara, CA 93106-9630, USA.

*E-mail address:* [lharrison@umail.ucsb.edu](mailto:lharrison@umail.ucsb.edu) (L.R. Harrison).

Pool–riffle sequences may also be found in mountain streams (Wohl, 2000), which are generally characterized by resistant channel boundaries, large roughness elements, and irregular flow patterns. In these high-gradient streams, pools are often “forced” by obstructions or channel constrictions (Lisle, 1986; Montgomery et al., 1995). Whereas a number of studies have addressed the maintenance of free-form pools found in alluvial channels, few have focused on the flow hydraulics of forced pools that are typical of boulder-bed streams. This study analyzed flow hydraulics through a forced pool–riffle sequence, to gain insight on the maintenance of these bedforms in boulder-bed streams.

### 1.2. Previous work

The study of pool–riffle sequences has been a focus in geomorphology for over 30 years and much progress has been made in terms of formation, maintenance and patterns of sediment transport (Keller, 1971; Clifford and Richards, 1992; Sear, 1996). The most widely utilized approach to studying the maintenance of pool–riffles has been based on the analysis of hydraulic parameters. Of the previously developed theories, the velocity reversal hypothesis proposed by Keller (1971) has received considerable attention. The velocity reversal hypothesis suggests that a hierarchical reversal exists in the magnitude of velocity over a riffle–pool sequence that acts to maintain the bed morphology. At low discharge, well below bankfull, the velocity in the riffle exceeds that in the pool. Relatively small bed material that moved out of the riffle is deposited in the adjacent pool. At high flow (at or near bankfull), the velocity of the pool exceeds that of the riffle. Thus, scour occurs in pools during these high flows and fill during low flow.

Many studies on pool–riffle sequences have tested the velocity reversal hypothesis, including Lisle (1979), O’Connor et al. (1986), Clifford and Richards (1992), Keller and Florsheim (1993), Carling and Wood (1994), Sear (1996), Thompson et al. (1998, 1999), Booker et al. (2001), Milan et al. (2001), Cao et al. (2003), MacWilliams (2004) and MacWilliams et al. (in press). Results from these studies show that while some pool–riffle sequences do exhibit a reversal in flow parameters, flow intensity may converge between pools and riffles as discharge increases but not necessarily reverse. Clifford and Richards (1992) suggested that the lack of agreement regarding the occurrence of flow reversals may result from local variations and complexity in pool–riffle morphology among field sites, as well as the diversity of parameters used to substantiate, reject or formulate alternative hypotheses. This problem is compounded by

the usage of cross-sectionally averaged data, which may mask non-uniform flow patterns within a transect. A lack of spatially distributed hydraulic data adds to the difficulty in determining the mechanism of pool–riffle maintenance (Booker et al., 2001).

In mountain channels with rough, irregular boundaries, pools are often forced by local obstructions, such as boulders, bedrock or debris jams (Keller and Swanson, 1979; Lisle, 1986; Montgomery et al., 1995; Montgomery and Buffington, 1997; Thompson et al., 1999). Roughness elements cause flow convergence, acceleration and enhanced capacity for sediment transport at high discharges, thus forcing the development of pools. In many coarse-grained, mountain rivers, pools formed by obstructions are the rule rather than the exception (Buffington et al., 2002).

Thompson et al. (1999) proposed a model for the maintenance of pool–riffles in coarse-bedded streams that relies upon channel constrictions creating flow convergence and high velocities through pools. According to this model, a velocity reversal is observed because of a recirculating eddy region and the development of a high velocity jet through the pool center. Patterns of scour and fill are controlled by convergent flow at the pool head and divergent flow over the pool-exit and downstream riffle.

The mechanisms which control forced pool–riffle morphology have received little attention, particularly for natural channels. The difficulty in observing scour in pools during relatively high magnitude, low frequency flows is one of the primary reasons that these channels have not been studied extensively. Channel conditions during floods commonly make direct field measurements hazardous or impossible. Consequently, computational hydraulic modeling offers an excellent opportunity to explore the relationships between channel hydraulics and processes thought to be important in maintaining forced pool–riffle sequences. Our study is one of the first to use a high-resolution two-dimensional model in a steep, boulder-bed channel. In this paper, we test the general hypothesis of velocity reversal (Keller, 1971), and the hypothesis of Thompson et al. (1999) who proposed that forced pool–riffle sequences in coarse-bedded streams are maintained by velocity or shear stress reversals caused by channel constrictions.

### 1.3. Hydraulic modeling

#### 1.3.1. One-dimensional modeling

The most widely used hydraulic models in geomorphology have been one-dimensional step-backwater models. These models have also been used extensively in applied projects on river restoration to assess channel

hydraulics. One-dimensional models, such as HEC-RAS (U.S. Army Corps of Engineers, 2001), are fixed-bed models that calculate the water surface depth and slope by solving the energy equation between cross-sections. The boundary conditions include cross-sectional geometry, water surface elevation, Manning's roughness, and an appropriate expansion/contraction coefficient. One-dimensional step-backwater models are capable of handling subcritical and supercritical flow and have been used in bedrock mountain channels more than any other type of model (Miller and Cluer, 1998; Wohl et al., 1999; Chin, 2003). These models have the advantage of making predictions over large spatial and temporal scales.

One-dimensional models can provide reconstruction of the cross-sectional distribution of hydraulic variables such as velocity, depth, and shear stress over a range of stream discharge values. These computations are useful in identification of maximum and minimum values of water surface slope and shear stress throughout the stream reach. This approach is well established and has been used successfully to address geomorphic questions by previous authors (O'Connor et al., 1986; Keller and Florsheim, 1993; Wohl et al., 1999; Chin, 2003). Nevertheless, these models should be used with caution in steep, mountain channels because they produce cross-sectionally averaged depth and velocity values and do not capture spatial trends in flow separation, recirculating eddies, or convergent or divergent flow.

### 1.3.2. Two-dimensional modeling

Two-dimensional flow modeling typically involves solution of the depth-integrated form of the conservation of mass and momentum equations. Input to the model includes topographic data, usually surveyed with a total station, boundary conditions for the water surface elevation, bed roughness, and an eddy viscosity value for turbulence closure. The output of the model includes depth and the downstream and transverse velocity vectors at each node in the flow grid. Two-dimensional models have been used for sediment routing (Wiele et al., 1996; Wiele and Torizzo, 2005), investigation of geomorphic processes (Miller, 1995; Miller and Cluer, 1998; Rathburn and Wohl, 2003), and in the design of river restoration projects (Pasternack et al., 2004, in press; Wheaton et al., 2004a,b). Nelson et al. (2003) note several improvements gained in using two-dimensional flow models. Instead of predicting only the cross-sectionally averaged components of downstream velocity and bed stress, these models predict downstream velocity and bed stress at many points across the channel. This means that the model can explicitly treat sit-

uations with large cross-stream velocity gradients and flow separation. Two-dimensional models also allow prediction of cross-stream structure of the water surface elevation, which is important in channels that experience super-elevation of the water surface because of channel curvature or irregular boundaries (Nelson et al., 2003).

Flow in steep mountain streams is characterized by irregularities in the water surface that are not captured by one-dimensional models (Miller and Cluer, 1998). In forced pools, flow separation and recirculating eddies have been found to be important components of the flow field (Schmidt, 1990; Thompson et al., 1998, 1999; Wohl and Cenderelli, 2000; Wohl and Cenderelli, 2000; Rathburn and Wohl, 2003). Modeling flow in mountain streams can require simulation of flow around large roughness elements such as boulders or bedrock outcrops. In a study on ecologically significant flow variables, Crowder and Diplas (2000) found that a two-dimensional flow model was capable of simulating flow around boulder obstructions, which strongly influenced the velocity gradient and degree of flow convergence. The local effects of flow caused by large roughness elements would not be captured through a one-dimensional approach. Clearly, attempts to understand the interactions between complex topography and flow patterns in mountain streams require at least a two-dimensional model.

### 1.3.3. Three-dimensional modeling

Data requirements to run three-dimensional models are essentially equivalent to those of a two-dimensional model. A three-dimensional model, however, has three distinct advantages (Nelson et al., 2003). The first is the prediction of secondary flows, such as helical flow around a meander bend. The second model enhancement is the precise treatment of the momentum fluxes that vary in the vertical dimension. The third improvement is the treatment of non-hydrostatic effects, which can be significant in regions of steep topography or flow around obstructions, which are common in boulder-bed channels.

To assess the predictive capability between two-dimensional and three-dimensional approaches, Lane et al. (1999) performed a comparison of two-dimensional and fully three-dimensional models in a gravel-bed river with high relative roughness. They found that the three-dimensional model provided more reliable estimates of bed shear stress and other flow parameters. Evaluation of the three-dimensional model, however, revealed high sensitivity to minor variations in the bathymetry because of problems in specifying topographic complexity. In addition, the calibration in a three-dimensional model requires detailed measurements of the three-dimensional

velocity field using an acoustic Doppler velocimeter (ADV). Given the complex geometry of most boulder-bed channels and the inherent challenges in obtaining calibration data for three-dimensional models, two-dimensional models offer a promising approach to simulating flow in boulder-bed streams. Here, we examine the interaction between flow hydraulics, topography and pool–riffle maintenance in a typical boulder-bed stream using two-dimensional numerical modeling.

## 2. Field area

Mountain streams in the chaparral environment of southern California are distinguished from other steep mountain channels by the unique linkage between the fire-cycle, vegetation and sediment production (Florsheim et al., 1991). Hillside vegetation burns periodically with a return period of 30–50 years, creating dramatic increases in the flushing of sediment. During the decades between wildfires, much less sediment is mobilized. High magnitude debris flows, that occur every few hundred years or more, deliver large boulders to stream channels (Florsheim et al., 1991). The combination of large debris flow-delivered boulders and low

volumes of available finer gravel are characteristic of boulder-bed channels in southern California. While the focus of the present study is on streams of the chaparral, the results are applicable to other mountain streams with large roughness elements.

Data collection was completed on a 45 m study reach of Rattlesnake Creek, which is located in the Santa Ynez mountains, north of Santa Barbara, CA (Fig. 1). The basin has a drainage area of 8.2 km<sup>2</sup>. Rattlesnake Creek descends from an elevation of 1164 m near the crest of the Santa Ynez Mountains and enters Mission Creek at an elevation of approximately 150 m. Rattlesnake Creek is typical of many watersheds found in coastal southern California. The channel is deeply incised, either directly into bedrock or through deposits of coarse sediment that extend 1.5 to 5 m above the present thalweg. The bed sediment is very coarse and much of it is probably immobile, except during very high magnitude floods or debris flows (Best, 1989).

The geologic units encountered in the study area include Quaternary and Tertiary age sedimentary rocks of marine and non-marine origin. The Tertiary units in the drainage basin are: the Juncal shale, Matilija sandstone, Cozy Dell shale, Coldwater sandstone and Sespe

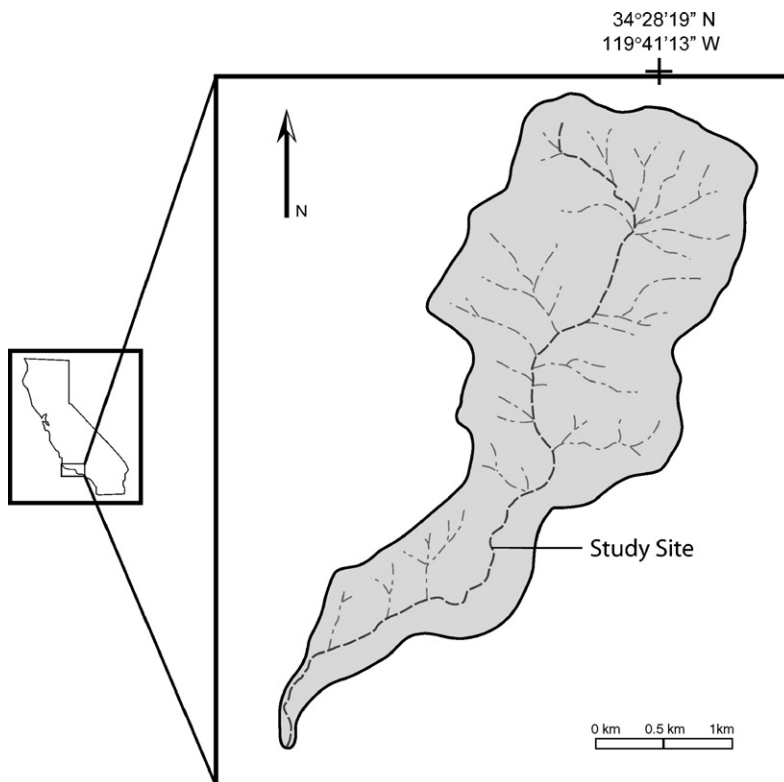


Fig. 1. Location map of Rattlesnake Creek near Santa Barbara, California.

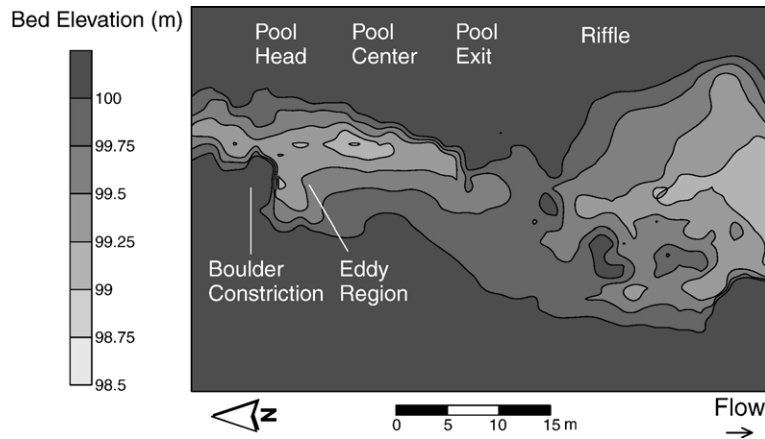


Fig. 2. Contour map of the study reach on Rattlesnake Creek illustrating boulder-constriction, pool and downstream riffle. Contour interval is 0.25 m.

sandstone (Dibblee and Ehrenspeck, 1986). The Juncal, Matilija, Cozy Dell and Coldwater formations are present in the upper Rattlesnake Creek drainage basin and serve as potential sediment sources.

Southern California has a Mediterranean climate with the majority of precipitation falling in the winter months. Rainfall–runoff relations are characterized by extreme runoff produced by intense rainfall over a short duration. Discharges typically have short lag times with peak flows lasting less than 1 h. The bankfull discharge at this site has been estimated at 5.0 m<sup>3</sup>/s based on bankfull indicators in the field and historical data (U.S. Army Corps of Engineers, 1984). Real-time data for flows are recorded using a pressure transducer, which is installed approximately 20 m below the stream reach.

These data were used for generating a local rating curve for the study site.

The study reach encompasses a forced pool–riffle sequence with a large boulder-constriction located directly above the pool (Fig. 2). The reach has a gradient of 0.02 (m/m) and is located roughly 10 m downstream from a step-pool sequence having a mean gradient of 0.04 (m/m). The study site is located in the Sespe sandstone and the large boulders found at the pool head are derived primarily from the Matilija and Coldwater sandstone. Alluvial deposits containing boulders 0.5 to 1 m in diameter are common throughout the riffle (Fig. 3), and field evidence suggests that boulders up to 2 m have been transported from source strata. Boulders greater than 2 m, along with protruding bedrock outcrops, exert significant



Fig. 3. Upstream view of riffle on Rattlesnake Creek.



Fig. 4. Upstream view of the pool on Rattlesnake Creek. Boulder large roughness element is outlined at the pool head.

local control over the formation of pools (Fig. 4). Additional channel attributes are listed in Table 1.

### 3. Methods

#### 3.1. Field measurements

##### 3.1.1. Channel topography

The primary data used in the flow modeling include channel topography, grain size and field measurements of depth and velocity at a known discharge. Capturing the three-dimensional topography allows for fine-scale flow calculations, which is especially important in channels with rough irregular boundaries. Detailed topography was surveyed with a total station including 1485 measurements over the 45 m reach. Individual boulders, bedrock outcrops, and breaks in slope were surveyed extensively. In areas of high boulder frequency, survey point density was 20 points/m<sup>2</sup>. Average point density over the reach was approximately 2.5 points/m<sup>2</sup>. A digital terrain model was computed from the topographic data by creating a triangulated irregular network (Fig. 5). The digital terrain model of the bed surface was used in the hydraulic calculations.

##### 3.1.2. Hydraulic data

Elevations of the water surface were surveyed at the wet/dry channel boundary during a discharge of approximately 2.5 m<sup>3</sup>/s. This was a sub-bankfull event equivalent to a flow with an approximate one-year return period (U.S. Army Corps of Engineers, 1984). During a

separate storm event (discharge of 0.5 m<sup>3</sup>/s), depth and velocity were measured at three cross-sections through the pool head, center and tail and over one longitudinal transect. All discharges in this study were determined from a stream gage located downstream from the study reach. Hydraulic data were collected on the falling limb of the hydrograph to avoid rapid fluctuations in discharge that can add error to the field measurements. Depth was measured with a stadia rod at 0.5 m intervals across the channel. Velocity readings were measured at 0.6 depth from the free surface using a Marsh McBirney electromagnetic current meter. Values for velocity were recorded every 6 s over a sixty second interval in both the downstream ( $U$ ) and transverse ( $V$ ) orientation. To match the position of measured and simulated data, surveyed data at the head pin of each transect were used to locate the nearest node within the computational mesh.

Table 1  
Study reach

Attributes of channel reach	Approximate physical dimensions
Channel-bed gradient*	0.02
Reach length	45.0 m
Constriction width	4.8 m
Pool width	10.0 m
Pool length	19.8 m
Maximum pool depth (moderate flow)*	1.1 m
Riffle width	14.6 m
Riffle length	17.4 m

\*Measured along channel thalweg.

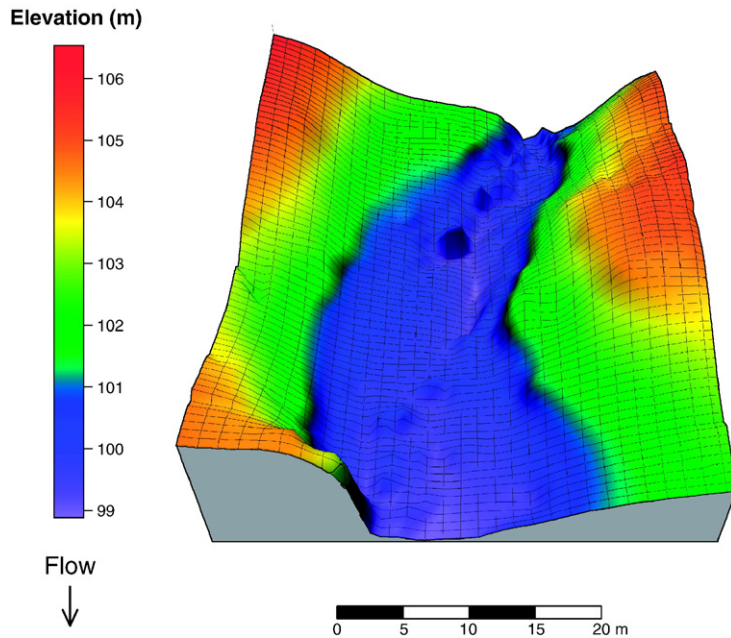


Fig. 5. Digital terrain model of the Rattlesnake Creek bed surface.

### 3.1.3. Sediment data

The distributions of grain sizes were measured in the study reach using a method of random pebble count (Wolman, 1954). Three separate surveys of grain sizes, consisting of 100 particles per survey, were conducted along several transects located in the pool center, pool exit, and the riffle. We observed distinct surficial patches of sediment in the pool, which were sampled separately to characterize the roughness of the bed.

Results from the sediment count are reported in Table 2. Based on this data, the coarsest particles were found on the downstream riffle, with a  $d_{50}$  value of 150 mm. Several cobble and small boulders (<300 mm) are found in the pool center though the bed material is predominantly gravels with a  $d_{50}$  of 28 mm. Bed material in the pool exit ranged from 4 to 60 mm with a  $d_{50}$  of 25 mm. The pool center and pool exit have similar median grain-sizes, while the coarse fraction ( $d_{90}$ ) in the pool center is nearly twice the value of the pool exit.

## 3.2. Flow modeling

### 3.2.1. Model description

To constrain the effects of large roughness elements on the flow hydraulics, River2D (Steffler and Blackburn, 2002) was selected. River2D is a two-dimensional hydrodynamic model that solves the depth-integrated form of the conservation of mass and momentum equations, using a finite element code. Input data include channel

bed topography, bed roughness, transverse eddy viscosity and initial flow conditions. A finite element mesh boundary was designed as an overlay on the digital terrain model and was refined to include greater detail in areas with high topographic complexity. Meshes had 1485 nodes and 2952 elements.

Elevations for the water surface were calculated in HEC-RAS, and then input into River2D as initial boundary conditions. The elevations of the water surface from HEC-RAS were compared with a stage-discharge relation developed from a pressure transducer that is installed approximately 20 m below the study reach. The pressure transducer is installed in a straight riffle with a similar gradient to that of the study reach. Elevations of the water surface, calculated in HEC-RAS, were calibrated by adjusting the Manning's  $n$  coefficient to bring the measured and observed values into agreement. Once calibrated, HEC-RAS simulations were used to set the boundary conditions required for construction of the River2D computational mesh.

Table 2  
Grain size distributions

Bedform	$d_5$	$d_{16}$	$d_{50}$	$d_{84}$	$d_{95}$
Pool center	12	16	28	42	90
Pool exit	9	11	25	40	48
Riffle	40	70	150	210	400

### 3.2.2. Model parameterization

Bed resistance was estimated based on the effective roughness height ( $k_s$ ). The grain roughness height  $k_s$  was estimated as 3.5 times the  $d_{84}$  for each morphologic environment (after Dietrich and Whiting, 1989). Model runs were performed with  $k_s$  values ranging from 1 to 4 times the  $d_{84}$  to test for the sensitivity of water surface elevation to different roughness configurations.

Elevations of the water surface did not show substantial changes with varying  $k_s$  height. This is likely because of the first-order effect of local topographic irregularity, which was accounted for in the digital terrain model. Values for roughness height were set explicitly at each node based on the grain size data. The  $k_s$  values used were 0.14 m in the pool exit, 0.17 m in the pool center and 0.96 m on the adjacent riffle.

To account for turbulence caused by bed shear, the eddy viscosity was calculated using a Boussinesq type eddy viscosity formulation (Steffler and Blackburn, 2002). Velocity was modeled using eddy viscosities ranging from 0.02 m<sup>2</sup>/s to 0.09 m<sup>2</sup>/s and compared to measured velocity data. An eddy viscosity of 0.05 m<sup>2</sup>/s provided the closest agreement with measured velocity data and was used in the final model runs.

### 3.2.3. Flow simulations

Model runs were performed for a range of flows to assess the spatial variation in velocity and shears stress with stage. Results from the River2D modeling provided depth-averaged velocity and depth at each node contained in the computational mesh. These output values were used to calculate bed shear stress over the study reach following Julien (1995). Determination of bed shear stress ( $\tau_b$ ) from data for depth-average velocity was calculated as:

$$\tau_b = \frac{\rho u^2}{\left[5.75 \log \left(12 \frac{H}{k_s}\right)\right]^2} \quad (1)$$

where:  $\rho$ =density of fluid;  $u$  is the depth-integrated velocity value from River2D;  $H$ =depth of flow and  $k_s$ =the roughness height. To assess changes in critical flow with stage, the Froude number ( $Fr$ ) was calculated over the study reach as:

$$Fr = \frac{u}{(gH)^{0.5}} \quad (2)$$

where:  $g$  is gravitational acceleration and  $u$  and  $H$  are as defined above in Eq. (1). The Froude number can be used to distinguish between subcritical flow ( $Fr < 1$ ), critical flow ( $Fr = 1$ ), and supercritical flow ( $Fr > 1$ ). Contour plots of bed shear stress and  $Fr$  were made using Surfer software over a range of high and low flow simulations.

The extent of flow convergence and divergence was quantified by identifying the effective width, defined here as the flow width which conveys 90% of the highest modeled velocities. This was done by removing the lowest 10% of the modeled velocity range for each discharge. For example, if the maximum modeled velocity for a given discharge was 3 m/s, to ascertain the effective width, we remove velocities below 0.3 m/s (the lowest 10%). The width of the remaining velocities across the channel represents an approximation of the effective width. The ratio of effective width between the pool and riffle was compared for low, moderate and high flows.

## 4. Results

### 4.1. Model calibration

Calibration of computer simulations with observed field data is an important step in the modeling process. Model calibration was performed using field measurements of depth, velocity and water surface elevation at two discharges. Comparison of calculated and observed water surface elevations was performed for a discharge of 2.5 m<sup>3</sup>/s. Least squares linear regression for measured and predicted values of water surface elevation on all points ( $n=19$ ) produced an  $r^2$  value of 0.84 and regression slope of 0.75. Matching of the edge of the water surface at this discharge significantly improved subsequent model predictions as it allowed for refinement in discretization of the computational mesh. Comparison of measured and predicted depth and velocity were made for a discharge of 0.5 m<sup>3</sup>/s. Reasonable agreement exists between measured and predicted depth, demonstrated by an  $r^2$  of 0.73 and a regression slope of 0.61 ( $n=22$ ), and an  $r^2$  of 0.84 and regression slope of 0.97 ( $n=16$ ) for measured and predicted velocity.

### 4.2. Depth-averaged velocity

To compare variations in shear stress and velocity with water stage, modeling was performed for three conditions: a low flow, bankfull discharge, and an estimated five-year flood. At a discharge of 0.5 m<sup>3</sup>/s (roughly 1/10th bankfull discharge), maximum velocities are estimated at 0.7 m/s and 1.2 m/s for the pool and riffle, respectively (Fig. 6a). Whereas a concentration of high velocity exists at the pool head, the higher velocity exists over the riffle. The region of zero velocity at the constriction represents the boulder roughness element which protrudes above the free surface at low and moderate discharges. Similarly, regions on the riffle showing zero velocity correspond to cobbles that

extend above the flow depth. Both regions are treated as dry nodes in the model solution.

During a discharge of 5.0 m<sup>3</sup>/s (approximate bankfull discharge), a peak velocity of 2.8 m/s is found at the pool head because of a constriction, while the maximum velocity over the riffle is estimated at approximately 2.5 m/s (Fig. 6b). Convergent flow created by the constriction is concentrated through the pool, creating a maximum velocity at the pool head. The jet is main-

tained by the recirculating eddy that develops below the boulder. Strong flow divergence can be seen on the pool exit. Flow entering the riffle shows divergent velocity contours but highly variable velocity vectors in response to coarse, irregular local topography.

The boulder-obstruction causes a backwater effect behind it, creating a steep water surface profile and a transverse pressure gradient towards the channel centerline. The cross-channel pressure gradient, caused by

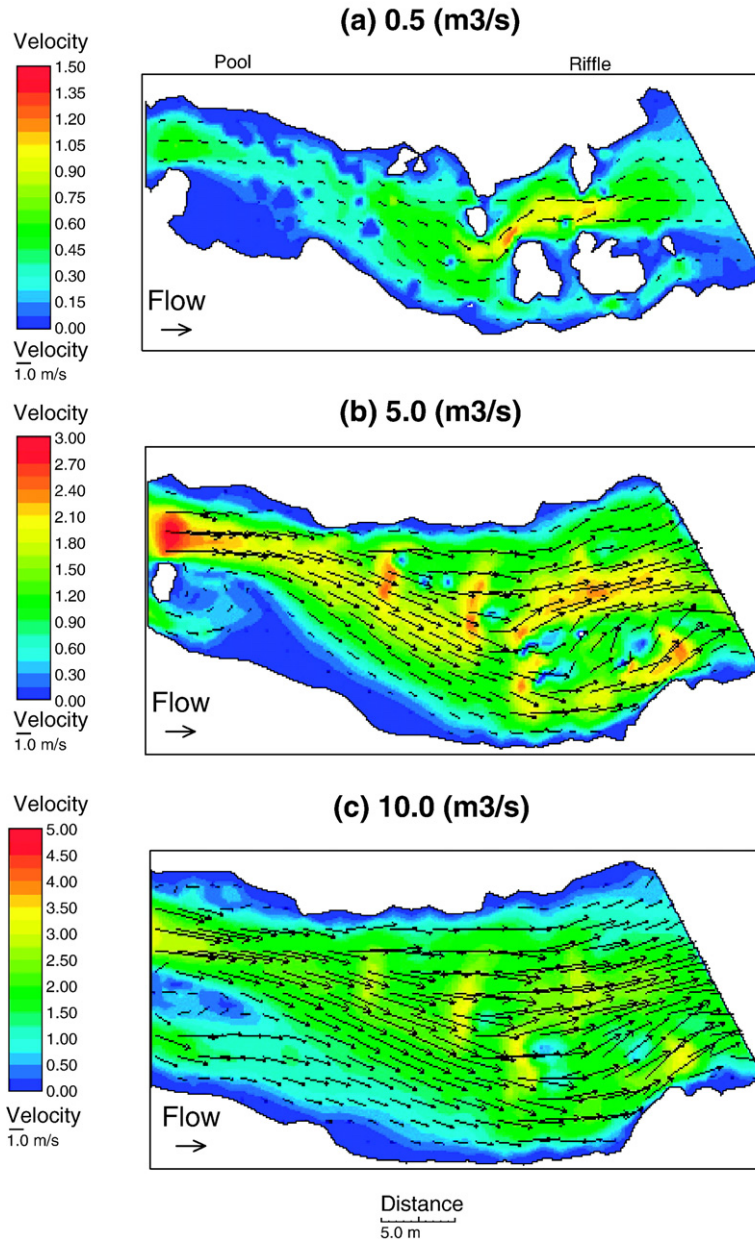


Fig. 6. Modeled velocity vectors overlain on velocity contour plots at discharges of: (a) 0.5 m<sup>3</sup>/s (approximately 10% of bankfull discharge), (b) 5.0 m<sup>3</sup>/s (approximate bankfull discharge), and (c) 10.0 m<sup>3</sup>/s (approximate five-year discharge).

the build-up of water behind the boulder, and the development of an eddy zone on the lee side of the boulder concentrates flow through the pool center. Thus, the high velocity core is steered by the channel topography. These model runs are consistent with results from [Thompson et al. \(1998, 1999\)](#) and with our field observations of the flow dynamics.

Simulations for a discharge of  $10 \text{ m}^3/\text{s}$  (approximate five-year flood), found that maximum velocities in the pool head and riffle tend to equalize at a value of approximately  $3.0 \text{ m/s}$  ([Fig. 6c](#)). Spatial trends in velocity vectors are similar to the bankfull event. Velocity contours, however, indicate more even distribution of velocity between the pool and riffle, reflecting the decreased ability of the boulder to converge flow into a single high velocity jet through the pool center.

#### 4.3. Shear stress

Values for shear stresses generally demonstrate the same trend as the modeled velocity predictions. At lower discharges, shear stress is greater over the downstream riffle than over the pool because of the low slope of the water surface ([Fig. 7a](#)). At approximately bankfull discharge, the shear stress maximum is concentrated at the pool head ([Fig. 7b](#)). Model results from the five-year flood indicate that the maximum values for shear stress are located over the submerged boulder found at the pool head, and over several cobble patches concentrated in the downstream riffle ([Fig. 7c](#)). During the five-year flood simulation, the predicted shear stress through the pool is lower than the values predicted by the bankfull simulation, reflecting the lack of convergence created by the boulder during the five-year flood.

Throughout all modeled runs, a high degree of spatial variability was found in the data for velocity and shear stress because of the complex topography. A cobble island exists on the right bank of the riffle that restricts flow to a narrow zone. In addition, surveying of individual cobbles and boulders over the riffle produces local highs of shear stress and velocity that may be an artifact of the modeling. Shear stress estimates, based on depth-averaged velocity, tend to provide overestimates of bed shear stress relative to three-dimensional predictions ([Lane et al., 1999](#)). Thus, we view the estimated shear stress as being representative of the spatial distribution, while the magnitude may be over-predicted.

#### 4.4. Critical flow

In a review of published data for the relation between channel gradient and Froude number, [Grant \(1997\)](#) found

that in hydraulically steep streams (gradients in excess of 0.01), mean Froude numbers were commonly close to unity. Modeling results from this study indicate that the Froude number increases through the pool and riffle with higher discharge, and values often exceed 1. For the simulations of low flow ([Fig. 8a](#)), the flow is subcritical throughout the reach but the most variability and the highest values are concentrated over the riffle. For bankfull flow ([Fig. 8b](#)), super critical flow is predicted at the pool head and downstream riffle. Model simulations for the five-year peak discharge ([Fig. 8c](#)) also predict super-critical flow over the pool and riffle.

## 5. Discussion

### 5.1. Model performance

In general, River2D reproduces the observed trends in depth and velocity throughout the modeled reach. Measured values of the elevations of the water surface at the wet/dry boundary during a discharge of  $2.5 \text{ m}^3/\text{s}$  were in reasonable agreement with predicted values. This was important in establishing the extent of the computational mesh. The closest agreement was in the pool center while the accuracy decreased on the margin of the high velocity core and the eddy, known as the eddy fence, because of the inability of the model to constrain the precise location of this transition. Measured values versus predicted values of  $r^2$  and regression slope reported here were within the range of other studies using computational hydraulic models, that report  $r^2$  values ranging from 0.51 to 0.77 and regression slopes ranging from 0.58 to 0.86 ([Booker et al., 2001](#) and [Lane et al., 1999](#)). Whereas these statistics provide comparison to other modeling studies, it is likely that the high topographic irregularity of the bed contributes greater error to the accuracy of the results than issues with the model. In our study, the availability of hydraulic field data was limited to two storms and a more extensive calibration data set would be required to assess errors created by assumptions in the model. The accuracy of future models could be improved through more detailed field measurements and an independent data set for validation of the model.

A limitation of using a depth-integrated model is the lack of information on the vertical velocity which can be important in sediment entrainment at high flows. In forced pools, the existence of a strong vertical velocity gradient near the constriction likely exists at high flows. The analogy of scour around bridge piers, summarized by [Melville \(1997\)](#), has been suggested as a mechanism for producing pool scour in channels with flow obstructions ([Lisle, 1986](#); [Thompson et al., 1998](#); [Buffington et al.,](#)

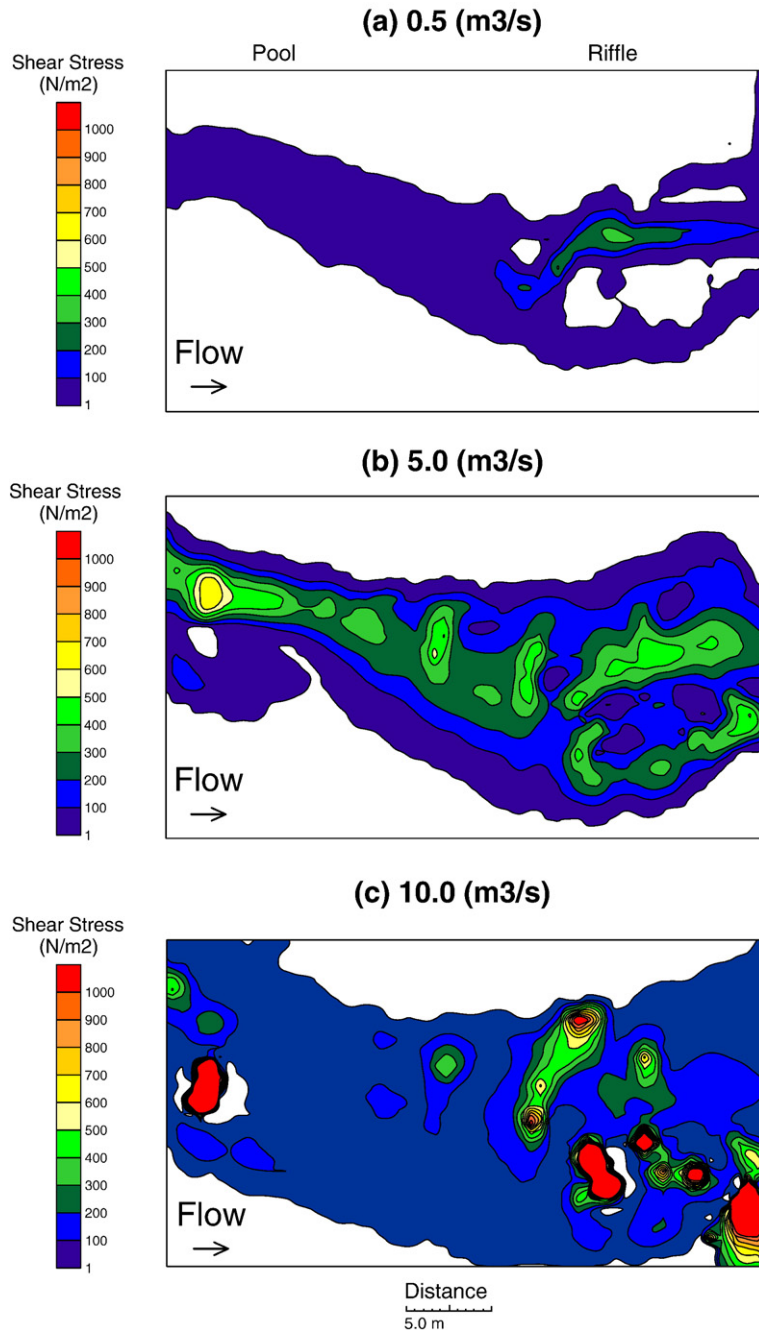


Fig. 7. Calculated shear stress distribution at discharges of: (a) 0.5 m<sup>3</sup>/s, (b) 5.0 m<sup>3</sup>/s and (c) 10.0 m<sup>3</sup>/s.

2002; Thompson, 2004). A common finding is that a vertical pressure gradient exists at the upstream face of the obstruction, causing downward flow, acceleration and the initiation of bed scour. In addition, the generation of vortices scours the bed by advecting high-velocity flow downward and mobilizing bed sediments (Thompson, 2004).

Using laboratory and field studies, Smith and Beschta (1994) found that vertical velocity profiles in pools with obstructions were irregular, reflecting a submerged jet. Because of strong downwelling below the constriction, the highest vertical velocity will likely be near the bed rather than at the 0.6 depth as assumed in a depth-integrated model. While a two-dimensional

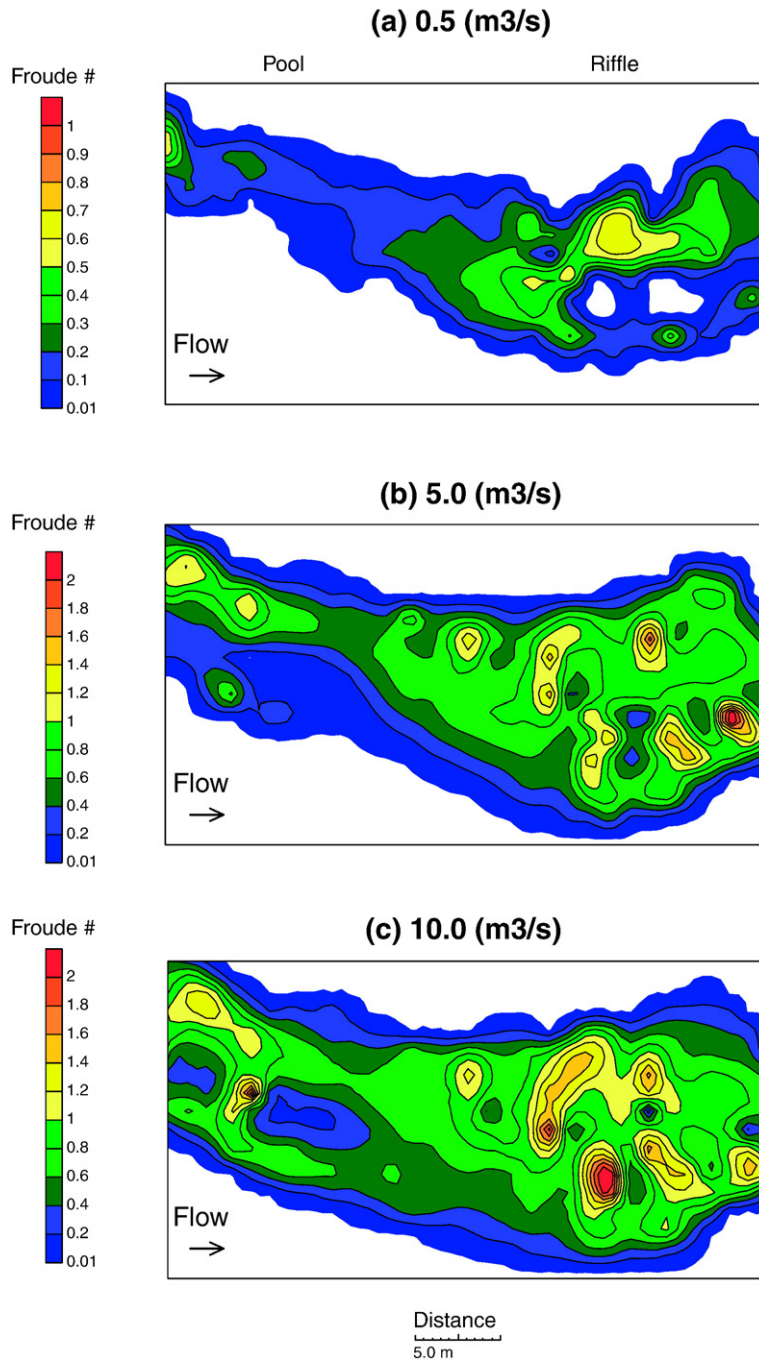


Fig. 8. Contour plot illustrating the spatial trends in the Froude number, based on model output for a discharge of: (a) 0.5 m<sup>3</sup>/s, (b) 5.0 m<sup>3</sup>/s and (c) 10.0 m<sup>3</sup>/s.

model cannot replicate vertical velocity gradients because of the assumption of hydrostatic pressure, it likely underpredicts magnitudes of velocity near constrictions because depth-averaged velocity is calculated at the 0.6 depth. Therefore, it is likely that the peak in

velocity and shear stress would remain at the pool head at high flows. To assess the validity of this assumption, further testing with three-dimensional flow data obtained with an acoustic Doppler velocimeter in conjunction with a three-dimensional model is required.

5.2. Bed roughness

Previous work by Carling and Wood (1994) found that a competence reversal (velocity, shear stress, shear velocity) could occur between pools and riffles when the bed material in the pool was coarser than that in the riffle. Thompson et al. (1998) also evoke the argument that coarser bed material in the pool can facilitate a reversal. The data from this study found that reversals in shear stress and velocity can occur in cases where the

grain size was significantly coarser in riffles than in pools. As Carling and Wood (1994) point out, flow reversals can occur because of differences in the channel width, which is in agreement with our data.

5.3. Effective width

Results from the flow modeling indicate that the reversal in depth-averaged velocity and shear stress is likely because of changes in cross-sectional width at

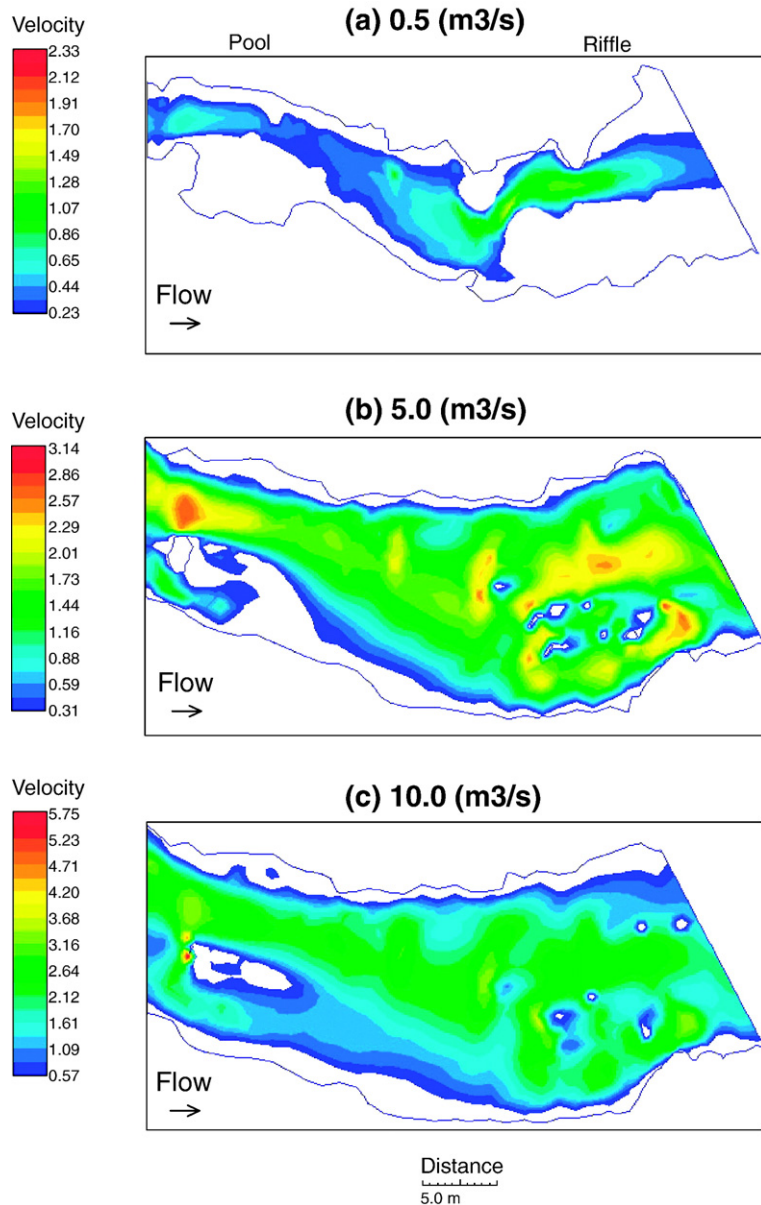


Fig. 9. Calculated effective flow width at discharges of: (a) 0.5 m<sup>3</sup>/s, (b) 5.0 m<sup>3</sup>/s and (c) 10 m<sup>3</sup>/s. The velocity contours shown represent the highest 90% of the modeled velocity data ( $V_{90}$ ). The dashed blue outline represents the wet/dry boundary if 100% of the flow is illustrated.

varying flows. Examination of the two-dimensional velocity contours in Figs. 6a–c demonstrates that only a portion of the flow is responsible for scouring bed material. Cherkauer (1973) proposed the concept of looking at the effective width of a pool–riffle sequence, which corresponds to the active extent of flow. More recently, Wilkinson et al. (2004) found that phase-shifts in shear stress between pool–riffle sequences were associated with variations in channel width at high flow.

After the dead water zone is eliminated, the lowest 10% of the velocity range, patterns of effective width begin to emerge. At low flow, the ratio of effective width between the pool and riffle is roughly 1:1, indicating little flow convergence or divergence (Fig. 9a). At bankfull discharge, the ratio of effective width is approximately 1:3 between the pool and downstream riffle illustrating the strong flow convergence at the pool head (Fig. 9b). The effective width tends to equalize with a ratio of 1:1 between the pool and riffle during a modeled discharge representing a five-year flood (Fig. 9c). In addition, the changes in the width of critical flow between the pool and riffle, shown in Fig. 8b and c, act to further highlight the trends in effective width.

A conceptual depiction of effective channel width, modified after the work of Thompson (2004), is shown in Fig. 10. The implication of the effective channel width is that only a portion of the channel will convey flow that is capable of scouring bed material. In pools, the effective width has been shown to vary with flow intensity and the size of adjacent eddies. As the eddy size increases, the effective flow width is confined to a thin high velocity jet as noted by Thompson et al. (1998, 1999), Rathburn and Wohl (2003) and Thompson (2004). The results from our modeling indicate that the size of the eddy region decreases at flows above bankfull

because of the inability of the boulder to converge flow. This trend highlights the observation made by Lisle (1986) that pool scour will vary in response to the constriction width. The trends in effective width observed on this reach reflect a specific morphology and drawing broader implications to other channels will require further testing using hydraulic modeling or laboratory flumes that have a superimposed pool–riffle morphology and scaled roughness elements.

#### 5.4. Maintenance of forced pool–riffle sequences

In Rattlesnake Creek, individual boulders within the channel constrict roughly 10%–50% of the active channel width and clearly influence flow hydraulics. Based on our flow simulations, the presence of the width constriction creates maximum velocities and shear stress at the pool head during bankfull discharge. This implies that pools are forced by boulders in a similar mechanism documented in streams with large woody debris (Keller and Swanson, 1979; Lisle, 1986; Montgomery et al., 1995). Pool formation in boulder-bed channels is commonly dependent upon the delivery of large boulders during landslides and debris flows, while the form appears to be maintained through flow convergence by the large roughness elements at roughly bankfull discharge.

Model results of a five-year flood indicate that the boulder is drowned out and is not able to converge flow into one high velocity core. During these events, a second high velocity zone is steered towards the point bar (Fig. 6c) and would likely change the asymmetric nature of the bar–pool morphology over time. If the bar were scoured during a large storm, it is likely that flow convergence through the pool would be diminished and higher flows would be required to cause pool scour.

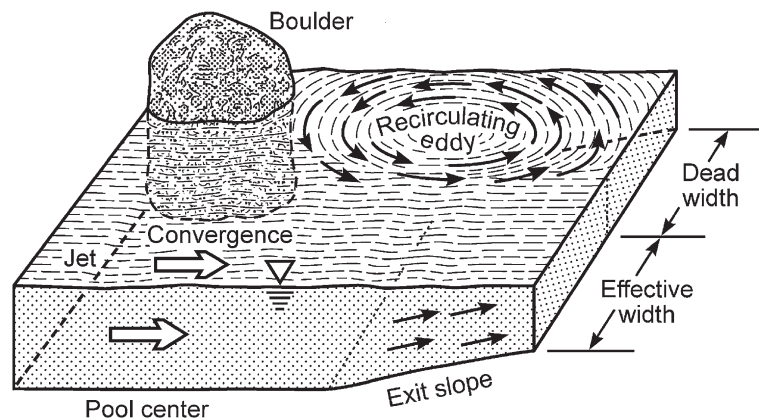


Fig. 10. Conceptual diagram showing effective width in a forced pool (modified after Thompson, 2004). Here the dead width represents areas of low velocity and potential deposition. Arrows represent the flow direction.

Simulation of the five-year flood highlights the limitations of using a fixed-bed model such as River2D. The discharge of  $10 \text{ m}^3/\text{s}$  would likely be able to entrain a large portion of the bed material, which could bury or dramatically alter the pool–riffle morphology. Thus, uncertainty exists in these predictions because the model assumes that the boundary conditions are stable, which may not be the case at this discharge. Despite the limitation inherent in this type of flow model, the simulated flow patterns suggest that forced pool–riffle sequence in boulder-bed streams are maintained primarily by flows with a return period of approximately 1–2 years.

Additional research pertaining to the maintenance of forced pool–riffle sequences in mountain streams would benefit from an enhanced characterization of the turbulent flow fields and sediment transport processes operating on these systems. This could include three-dimensional flow modeling to resolve the role of the vertical velocity component in bed scour. Three-dimensional velocity measurements using an acoustic Doppler velocimeter over a range of discharges, either in natural channels or scaled laboratory flumes, would also help in assessing the role of turbulent fluctuations in shaping pool–riffle sequences.

The results from this model indicate that riffles exhibit higher bed stress and more extensive regions of critical flow (defined by the  $F_r$ ) at low stage. It follows that the bed particles on the riffle likely experience more turbulent flow during low magnitude, high frequency events. As noted by Sear (1996), the bed surface on riffles can become more tightly packed under these conditions and necessitate higher entrainment thresholds than pools. Recent advances in the predictions of sediment transport in steep boulder-bed channels (Yager et al., 2002), and improved understanding of the role of large roughness elements on flow and sediment transport (Yager et al., 2004), could be used to test if the phenomenon observed by Sear (1996) occurs in boulder-bed streams. A more complete model of flow, sediment transport, and morphodynamics could be gained through a coupled model of flow and sediment transport, to further refine hypotheses on the maintenance of forced pool–riffle sequences in boulder-bed streams.

## 6. Conclusion

This study supports the general hypothesis of velocity reversal (Keller, 1971) and also the model of pool maintenance in forced pools proposed by Thompson et al. (1999). Results from the hydraulic model indicate that at low discharge, a peak zone of shear stress and velocity exists over the riffle. At or near bankfull discharge, the peak in velocity and shear stress is found at the pool head

because of strong flow convergence created by large roughness elements. The extent of flow convergence and divergence was quantified by identifying the effective width, defined here as the flow width which conveys 90% of the highest modeled velocity. At low flow, the ratio of effective width between the pool and riffle is roughly 1:1, indicating little flow convergence or divergence. At bankfull discharge, the ratio of effective width is approximately 1:3 between the pool and downstream riffle, illustrating the strong flow convergence at the pool head. The effective width tends to equalize with a ratio of 1:1 between the pool and riffle during a modeled discharge representing a five-year flood. These results suggest that forced pools in boulder-bed streams are maintained by flows at or near bankfull discharge because of stage-dependent variability in flow competency and the effective channel width.

## Acknowledgements

This work was supported by a University of California Academic Senate Grant and funding from the Geological Society of America. Numerous individuals helped with the field data collection including Carl Legleiter, Garret Bean, Matt Sallee, Heidi Schott and Marlene Duffy. We appreciate improvements to an earlier version of the manuscript suggested by Anne Chin, Vincenzo D'Agostino and an anonymous reviewer. River2D is produced and made available by Peter Steffler and Julia Blackburn, Department of Civil and Environmental Engineering, University of Alberta, Canada.

## References

- Best, D.W., 1989. Sediment storage and routing in a steep, boulder-bed rock-controlled channel, near Santa Barbara, California. M.S. Thesis, University of California at Santa Barbara, 162 pp.
- Booker, D.J., Sear, D.A., Payne, A.J., 2001. Modeling three-dimensional flow structures and patterns of boundary shear stress in a natural pool–riffle sequence. *Earth Surface Processes and Landforms* 26, 553–576.
- Buffington, J.M., Lisle, T.E., Woodsmith, R.D., Hilton, S., 2002. Controls on the size and occurrence of pools in coarse-grained forest rivers. *River Research and Applications* 18, 507–531.
- Cao, Z., Carling, P.A., Oakey, R., 2003. Flow reversal over a natural pool–riffle sequence: a computational study. *Earth Surface Processes and Landforms* 28, 689–705.
- Carling, P.A., Wood, N., 1994. Simulation of flow over pool–riffle topography: a consideration of the velocity reversal hypothesis. *Earth Surface Processes and Landforms* 19, 319–332.
- Cherkauer, D.S., 1973. Minimization of power expenditure in a riffle–pool alluvial channel. *Water Resources Research* 9, 1613–1628.
- Chin, A., 2003. The geomorphic significance of step-pools in mountain streams. *Geomorphology* 55, 125–137.
- Clifford, N.J., Richards, K., 1992. The reversal hypothesis and the maintenance of riffle–pool sequences: a review and field appraisal.

- In: Carling, P., Petts, G. (Eds.), *Lowland Floodplain Rivers: Geomorphological Perspectives*. John Wiley and Sons Ltd, Chichester, U.K., pp. 43–70.
- Crowder, D.W., Diplas, P., 2000. Using two-dimensional hydrodynamic models at scales of ecological importance. *Journal of Hydrology* 230, 172–191.
- Dibblee, T.W., Ehrenspeck, H.E., 1986. Geologic map of the Santa Barbara quadrangle, Santa Barbara County, California. Dibblee Geological Foundation, Map DF-06.
- Dietrich, W.E., Whiting, P.J., 1989. Boundary shear stress and sediment transport in river meanders of sand and gravel. In: Ikeda, S., Parker, G. (Eds.), *River Meandering*. Water Resources Monograph, vol. 12, pp. 1–50.
- Florsheim, J.A., Keller, E.A., Best, D.W., 1991. Fluvial sediment transport in response to moderate storm flows following chaparral wildfire, Ventura County, Southern California. *Geological Society of America Bulletin* 103, 504–511.
- Grant, G.E., 1997. Critical flow constrains flow hydraulics in mobile-bed streams: a new hypothesis. *Water Resources Research* 33, 349–358.
- Julien, P.Y., 1995. *Erosion and sedimentation*. Cambridge University Press, New York. 280 pp.
- Keller, E.A., 1971. Areal sorting of bed-load material: the hypothesis of velocity reversal. *Geological Society of America Bulletin* 82, 753–756.
- Keller, E.A., Swanson, F.J., 1979. Effects of large organic material on channel form fluvial processes. *Earth Surface Processes* 4, 361–380.
- Keller, E.A., Florsheim, J.L., 1993. Velocity- reversal hypothesis: a model approach. *Earth Surface Processes and Landforms* 18, 733–748.
- Lane, S.N., Bradbrook, K.F., Richards, K.S., Biron, P.A., Roy, A.G., 1999. The application of computational fluid dynamics to natural river channels: three dimensional versus two-dimensional approaches. *Geomorphology* 29, 1–20.
- Lisle, T.E., 1979. A sorting mechanism for a pool–riffle sequence: summary. *Geological Society of America Bulletin* 90, 616–617.
- Lisle, T.E., 1986. Stabilization of a gravel channel by large streamside obstructions and bedrock bends, Jacoby Creek, northwestern California. *Geological Society of America Bulletin* 97, 999–1011.
- MacWilliams, M.L., 2004. Three-dimensional hydrodynamic simulation of river channels and floodplains. PhD Dissertation, Stanford University, Stanford, California, 222 pp.
- MacWilliams, M.L., Wheaton, J.M., Pasternack, G.B., Kitanidis, P.K., Street, R. L. in press. The flow convergence–routing hypothesis for pool–riffle maintenance in alluvial rivers. *Water Resources Research*.
- Milan, D.J., Heritage, G.L., Large, A.R.G., Charlton, M.E., 2001. Stage dependent variability in tractive force distribution through a riffle–pool sequence. *Catena* 44, 85–100.
- Melville, B.W., 1997. Pier and abutment scour: integrated approach. *Journal of Hydraulic Engineering* 123, 125–136.
- Miller, A.J., 1995. Valley morphology and boundary conditions influencing spatial patterns of flood flow. In: Costa, J.E., Miller, A.J., Potter, K.W., Wilcok, P.R. (Eds.), *Natural and Anthropogenic Influences in Fluvial Geomorphology: The Wolman Volume*. American Geophysical Monograph, pp. 57–81.
- Miller, A.J., Cluer, B.L., 1998. Modeling considerations for simulation of flow in bedrock channels. In: Tinkler, K.J., Wohl, E.E. (Eds.), *Rivers over rock: Fluvial processes in bedrock channels*. American Geophysical Monograph, vol. 107, pp. 61–104.
- Montgomery, D.R., Buffington, J., 1997. Channel-reach morphology in mountain drainage basins. *Geological Society of America Bulletin* 109, 596–611.
- Montgomery, D.R., Buffington, J.M., Smith, R.D., Schmidt, K.M., Pess, G., 1995. Pool spacing in forest channels. *Water Resources Research* 31, 1097–1105.
- Nelson, J.M., Bennett, J.P., Wiele, S.M., 2003. Flow and sediment transport modeling. In: Kondolf, G.M., Piegay, H. (Eds.), *Tools in Fluvial Geomorphology*. Wiley, West Sussex, England.
- O'Connor, J.E., Webb, R.H., Baker, V.R., 1986. Paleohydrology of pool and riffle pattern development; Boulder Creek, Utah. *Geological Society of America Bulletin* 97, 410–420.
- Pasternack, G.B., Wang, C.L., Merz, J.E., 2004. Application of a 2D hydrodynamic model to design of reach-scale spawning gravel replenishment on the Mokelumne River, California. *River Research and Applications* 20, 205–225.
- Pasternack, G.B., Gilbert, A.T., Wheaton, J.M., Buckland, E.M., in press. Error propagation for velocity and shear stress predictions using 2D models for environmental management. *Journal of Hydrology*.
- Rathburn, S., Wohl, E.E., 2003. Predicting fine sediment dynamics along a pool–riffle mountain channel. *Geomorphology* 55, 111–124.
- Schmidt, J.C., 1990. Recirculating flow and sedimentation in the Colorado River in Grand Canyon, Arizona. *Journal of Geology* 98, 709–724.
- Sear, D.A., 1996. Sediment transport processes in pool–riffle sequences. *Earth Surface Processes and Landforms* 21, 241–262.
- Smith, R.D., Beschta, R.L., 1994. A mechanism of pool formation and maintenance in forest streams. *Proceedings of the 1994 ASCE Hydraulic Engineering Conference*. Buffalo, New York.
- Steffler, P., Blackburn, J., 2002. *Two-Dimensional Depth Averaged Model of River Hydrodynamics and Fish Habitat: River2D User's Manual*. University of Alberta, Canada.
- Thompson, D.M., 2004. The influence of pool length on local turbulence production and energy slope: a flume experiment. *Earth Surface Processes and Landforms* 29, 1341–1358.
- Thompson, D.M., Nelson, J.M., Wohl, E.E., 1998. Interactions between pool geometry and hydraulics. *Water Resources Research* 34, 3673–3681.
- Thompson, D.M., Wohl, E.E., Jarrett, R.D., 1999. Velocity reversals and sediment sorting in pools and riffles controlled by channel constrictions. *Geomorphology* 27, 229–241.
- U.S. Army Corps of Engineers, 2001. *HEC-RAS Users Manual*. Hydrologic Engineering Center, Davis, California.
- U.S. Army Corps of Engineers, 1984. *Debris deposition study for without-project and with-project conditions, Santa Barbara County streams Mission Creek and Rattlesnake Creek*. Newport Beach, CA.
- Wheaton, J.M., Pasternack, G.B., Merz, J.E., 2004a. Spawning habitat rehabilitation—I. Conceptual approach and methods. *Journal of River Basin Management* 2, 3–20.
- Wheaton, J.M., Pasternack, G.B., Merz, J.E., 2004b. Spawning Habitat Rehabilitation—II. Using hypothesis development and testing in design, Mokelumne River, California, U.S.A. *Journal of River Basin Management* 2, 21–37.
- Wiele, S.M., Torizzo, M., 2005. Modelling of sand deposition in archaeologically significant reaches of the Colorado River in Grand Canyon, USA. In: Bates, P.D., Lane, S.N., Ferguson, R.I. (Eds.), *Computational Fluid Dynamics: Applications in Environmental Hydraulics*. John Wiley and Sons, pp. 357–394.
- Wiele, S.M., Graf, J.B., Smith, J.D., 1996. Sand deposition in the Colorado River in the Grand Canyon from flooding of the Little Colorado River. *Water Resources Research* 32, 3579–3596.

- Wilkinson, S.N., Keller, R.J., Rutherford, I.D., 2004. Phase-shifts in shear stress as an explanation for the maintenance of pool–riffle sequences. *Earth Surface Processes and Landforms* 29, 737–753.
- Wohl, E.E., 2000. Mountain rivers. American Geophysical Union, *Water Resources Monograph*, vol. 14. 320 pp.
- Wohl, E.E., Cenderelli, D., 2000. Sediment deposition and transport patterns following a reservoir sediment release. *Water Resources Research* 36, 319–333.
- Wohl, E.E., Thomson, D.M., Miller, A.J., 1999. Canyons with undulating walls. *Geological Society of America Bulletin* 111, 949–959.
- Wolman, M.G., 1954. A method of sampling coarse river-bed material. *Eos Transactions, American Geophysical Union* 35, 951–956.
- Yager, E., Kirchner, J.W., Dietrich, W.E., Furbish, D.J., 2002. Prediction of sediment transport in steep boulder-bed channels. *EOS Trans. AGU Fall Meet. Suppl.* 83 (47) Abstract H21G-03.
- Yager, E., Schmeeckle, M., Dietrich, W.E., Kirchner, J.W., 2004. The effect of large roughness elements on local flow and bedload transport. *Eos Trans. AGU Fall Meet. Suppl.* 85 (47) Fall Meet. Suppl., Abstract H41G-05.